BEAM COUPLING IMPEDANCE MODELING FOR THE HEFEI ADVANCED LIGHT FACILITY *

T. He†, W. Li, X. Liu, Z. Bai, G. Feng, University of Science and Technology of China, Hefei, China

Abstract

The Hefei Advanced Light Facility (HALF), which is being built as a 4th-generation synchrotron light source, faces performance challenges directly from instabilities associated with beam coupling impedance. This paper presents a systematic impedance modeling study based on two computational campaigns, establishing both narrow-band and broad-band impedance budgets. Key impedance sources are identified, informing targeted optimization and mitigation strategies. The resulting model enables a comprehensive analysis of impedance-driven beam dynamics for the HALF storage ring.

INTRODUCTION

Geometric discontinuities in vacuum components generate beam coupling impedance, classified into broad-band and narrow-band types. Broad-band impedance, from rapidly decaying wakefields, affects single-bunch dynamics and sets the single-bunch current threshold. Narrow-band impedance, from slowly decaying trapped-mode wakefields, drives multi-bunch instabilities and limits the total average current [1–4]. Both effects are critical for the HALF storage ring [5]. For convenience, key vacuum components are grouped into five functional systems: (1) RF system (main and harmonic cavities); (2) insertion devices (IDs): long (4.2 m) and short (1.1 m) in-vacuum undulators (IVUs), plus tapered transitions for out-vacuum undulators (OVUs); (3) vacuum mechanical system: photon masks, gate valves, four RF-shielded bellows; (4) beam diagnostics: 240 BPM-bellow blocks, 7 stand-alone BPMs, collimators, feedback kickers, tune striplines, current monitor; (5) injection system: nonlinear kicker, septum, dual-channel kicker.

Two computational campaigns were performed using the CST Wakefield Solver [6], except for the main and harmonic cavities which were modeled with ECHO2D [7]. The first campaign targeted narrow-band trapped modes. For most components, a bunch length of 5 mm and a wake length of 10 m were used, with a frequency range up to 20 GHz. For large structures such as IVUs, where critical trapped modes lie in the hundred-MHz range, a longer bunch length of 50 mm was adopted, with a frequency range up to 2 GHz. For incompletely decaying wakes, a Particle Swarm Optimization (PSO) fitting method was used to extract trapped-mode parameters [8], i.e., the resonant frequency f_r, shunt impedance R, and quality factor Q. The second campaign addressed broad-band impedance up to 200 GHz using a bunch length of 0.5 mm and a wake length of 300 mm. The resulting short-range wakes form the basis for the impedance budget and single-bunch instability tracking simulations.

* Work supported by the Fundamental Research Funds for the Central Universities (No. WK2310000127) and the National Natural Science Foundation of China (Grants No. 12375324 and No. 12105284).

† htlong@ustc.edu.cn

NARROW-BAND IMPEDANCE

Tables 1, 2, and 3 summarize the most significant trapped modes for the longitudinal, horizontal, and vertical planes, respectively. The trapped modes in each table are listed in order of increasing frequency.

In the longitudinal plane (Table 1), the gate valves exhibit the most significant trapped modes, both in terms of total aggregate impedance and per-unit contribution. With 40 units installed throughout the ring, the mode at 7746 MHz alone contributes a total shunt impedance of 114.1 kΩ, an order of magnitude larger than any other component. This is primarily due to the cavity-like geometry of the gate valve structure, which supports high-Q resonances. The BPM-bellow blocks, with 200 units, also contribute substantially through multiple modes across the frequency spectrum. Notably, near 8.7 GHz and 19 GHz, multiple trapped modes with relatively high Q-factors and large cumulative impedances are observed, which can be primarily attributed to the common and similar bellow structures present in these components.

For the horizontal plane (Table 2), the collimators represent the dominant impedance sources. Despite having only two units, the horizontal collimators exhibit very high transverse shunt impedances, with the mode at 4228 MHz reaching $\beta R_t = 6.05$ MΩ. The BPM-bellow blocks, while having lower per-unit impedances, contribute significantly due to their large population of 200 units, particularly the high-Q mode at 13 879 MHz, which accumulates to $\beta R_t = 13.1$ MΩ.

The vertical plane (Table 3) presents the most severe impedance challenges. The long IVU exhibits two ultra-low-frequency modes at approximately 27 MHz and 56 MHz with extremely high transverse shunt impedances, $\beta_y R_t = 257$ MΩ and 81 MΩ, respectively. The short IVU also contributes two strong modes at 57 MHz and 226 MHz, with $\beta_y R_t = 119$ MΩ and 23.2 MΩ. These modes arise from the ridge-waveguide-like structure of the IVUs, and their impedance characteristics are highly dependent on the magnetic gap. The NLK contributes a significant mode at 1564 MHz with $\beta_y R_t = 14.3$ MΩ. The BPM-bellow blocks again show a strong cumulative effect, with the high-Q mode at 13 879 MHz accumulating to nearly 20 MΩ. These vertical plane impedances, particularly the IVU modes, are expected to pose the greatest risk for multi-bunch instabilities.

Table 1: Important Longitudinal Trapped Modes

Elements	N_{elem}	f_r [MHz]	R/Q [Ω]	Q	R [Ω]	$R \times N_{elem}$ [kΩ][4]
Main cavity	1	993	2.86	497	1425	1.4
Harmonic cavity	1	4378	–	–	1466	1.5
Gate Valve[1]	40	7746	0.389	7325	2853	114.1
Harmonic cavity	1	8074	–	–	1550	1.6
LSN-MSK02	20	8711	0.123	1843	227	4.5
RCN-VC21	20	8732	0.172	1118	192	3.8
BPM-**Bellow**[2]	200	8756	0.143	2419	347	69.4
Gate Valve[1]	40	8777	0.243	1318	320	12.8
BPM[3]	247	15260	0.039	775	30	7.4
BPM[3]	247	17167	0.135	277	38	9.4
Gate Valve[1]	40	19002	0.028	5310	149	6.0
BPM-**Bellow**[2]	200	19896	0.032	3892	127	25.4

[1] The gate valve, together with LSN-MSK01 and the bellow component of the BPM-bellow blocks, is modeled as a combined structure, and is simply denoted as "Gate Valve" in the table. Consequently, this model shares the same bellow structure as the BPM-bellow blocks, which explains the remarkably similar trapped mode impedances observed between them, e.g., around 8.8 GHz and 19 GHz.

[2] The gray-colored "BPM" and bold "Bellow" indicate that the trapped modes originate specifically from the bellow structure.

[3] All BPMs are modeled individually without considering the influence of adjacent bellows.

[4] When summing the total impedance, all trapped modes are assumed to be perfectly aligned in frequency. In practice, frequency mismatches may exist due to slight dimensional variations among components arising from manufacturing and installation tolerances, and this assumption tends to overestimate their collective impact.

Table 2: Important Horizontal Trapped Modes

Elements	N_{elem}	f_r [MHz]	R_t/Q [Ω/m]	Q	R_t [kΩ/m]	$\beta_x R_t \times N_{elem}$ [kΩ]
TFBK-V	1	3825	74.1	1711	126.8	936
Collimator-H	2	4228	667.0	825	549.9	6049
Collimator-H	2	4717	323.1	729	235.6	2592
Collimator-H	2	5302	185.2	606	112.2	1234
LSN-MSK02	20	6334	5.625	1646	9.26	1287
BPM-**Bellow**	200	6841	3.893	287	1.12	1001
LSN-MSK02	20	13744	2.154	1695	3.65	508
BPM-**Bellow**	200	13879	2.077	7063	14.67	13144
Gate Valve	40	13891	4.669	3073	14.30	2711

Table 3: Important Vertical Trapped Modes

Elements	N_{elem}	f_r [MHz]	R_t/Q [Ω/m]	Q	R_t [kΩ/m]	$\beta_y R_t \times N_{elem}$ [kΩ]
IVU-long[1]	1	27	249000	331	82430	257180
IVU-long[1]	1	56	93500	277	25950	80960
IVU-short[1]	1	57	196000	291	57000	119000
IVU-short[1]	1	226	28200	393	11100	23200
NLK	1	1564	3461.1	1193	4129	14328
OVU taper	11	1591	88.8	1931	171.5	5886
Collimator-V	1	3964	650.3	767	498.9	4740
Collimator-V	1	4479	587.7	716	420.6	3996
LSN-MSK02	20	6334	5.625	1646	9.26	557
Collimator-V	1	6763	660.2	659	435.3	4135
BPM-**Bellow**	200	6841	3.893	287	1.12	1522
RCN-VC21	20	13790	2.269	1513	3.43	975
BPM-**Bellow**	200	13879	2.077	7063	14.67	19980
Gate Valve	40	13891	4.669	3073	14.30	4347

[1] The IVU models incorporate the pumping ports, which significantly affect the trapped mode characteristics.

BROAD-BAND IMPEDANCE

The broad-band impedance budget is presented in Table 4, showing the loss factor, effective impedance, and kick factors for both the natural bunch length of 2 mm and the case with a threefold bunch length stretching.

Table 4: Broad-Band Impedance Budget for HALF

Components	No.	Code	β_x	β_y	@ 2 mm RMS bunch length				@ 6 mm RMS bunch length			
			[m]	[m]	κ_z [V/pC]	$\mathrm{Im}Z_{\mathrm{eff}}/n$ [mΩ]	$\beta\kappa_x$ [V/pC]	$\beta\kappa_y$ [V/pC]	κ_z [V/pC]	$\mathrm{Im}Z_{\mathrm{eff}}/n$ [mΩ]	$\beta\kappa_x$ [V/pC]	$\beta\kappa_y$ [V/pC]
Main cavity	1	ECHO2D	6.82	2.67	7.34	9.81	393.3	154.0	1.670	25.64	161.1	63.1
Harmonic cavity	1	ECHO2D	2.63	2.1	4.62	5.07	125.4	100.1	0.751	10.18	56.7	45.3
Long-IVU	1	CST	6.82	2.67	2.44	3.85	1128.5	1007.2	0.191	5.47	436.7	587.5
Short-IVU	1	CST	2.63	2.1	2.60	4.05	505.6	928.7	0.210	5.80	196.6	526.1
OVU-taper	11	CST	6.99	3.12	0.79	6.86	1907.5	3711.9	0.006	6.59	617.6	1793.8
Gate-Valve and its neighbors	40	CST	7.6	4.74	3.99	9.67	2216.9	1382.6	0.386	13.75	919.9	573.8
Bellow: LSN-MSK02	20	CST	6.95	3.01	0.37	0.83	210.9	91.3	0.043	1.35	92.3	39.4
Bellow: RCN-VC21	20	CST	1.62	14.6	0.84	1.30	153.1	1379.5	0.033	1.54	59.5	536.5
Bellow: RCN-MSK01	20	CST	4.76	10.52	0.51	1.31	145.3	321.2	0.042	1.70	60.2	133.0
Photon Masks	248	CST	–	–	5.54	10.45	2337.0	1434.4	0.371	13.95	1132.1	553.0
BPM(240+7)-Bellow	247	CST	4.25	6.63	2.49	4.43	632.5	986.8	0.126	5.73	277.3	432.7
BPM-Bellow(240-40)	200	CST	4.48	6.81	4.64	11.41	1774.0	2696.7	0.432	16.47	725.5	1103.5
TFBK-H & V	1	CST	7.38	4.16	1.04	1.15	315.2	171.0	0.338	3.33	309.9	167.9
Tune-SBPM + Kicker	2	CST	5.34	9.78	0.57	0.59	58.9	216.7	0.105	1.43	49.8	168.5
LFBK-Kicker	1	CST	2.83	2.35	0.98	0.93	72.1	59.8	0.418	3.47	63.2	52.5
Bunch Current Monitor	1	CST	5.34	9.78	0.30	0.27	57.8	105.9	0.109	0.97	62.9	115.1
Collimator-H	2	CST	5.5	9.5	0.35	1.09	645.6	475.6	0.040	1.331	274.9	168.0
Collimator-V	1	CST	5.5	9.5	0.24	1.42	634.1	1799.6	0.009	1.43	218.9	835.7
Non-linear kicker	1	CST	7.12	3.47	0.17	0.91	955.2	372.0	0.003	0.90	320.9	172.2
Dual-channel kicker	1	CST	7.12	3.47	0.57	0.98	332.6	62.0	0.059	1.44	162.9	30.9
Septum	1	CST	7.12	3.47	0.67	0.86	224.6	41.6	0.113	1.72	152.5	22.6
Sum					**41.06**	**77.24**	**14827**	**17499**	**5.46**	**124.19**	**6351.4**	**8121.1**

Among the various components, the RF cavities, gate valves, BPM-bellow blocks, and photon masks contribute most significantly to the loss factor and effective longitudinal impedance. For the transverse planes, the IVUs, OVU tapers, photon masks, BPM-bellow blocks, collimators, and gate valves are the dominant contributors to the kick factors, with the IVUs and OVU tapers showing particularly strong vertical contributions. Bunch length stretching by a factor of three substantially reduces the total loss factor from 41.06 V/pC to 5.46 V/pC, approximately one order of magnitude, and more than halves the transverse kick factors, albeit with an increase in the longitudinal effective impedance from 77.24 mΩ to 124.19 mΩ. This budget provides a direct reference for evaluating the relative impedance contributions of individual geometric components, clearly illustrating the dominant contributors. Furthermore, it demonstrates the significant effect of bunch length stretching by the harmonic cavity in reducing impedance-induced power deposition.

Figure 1 compares the total geometric wake potential with the resistive wall (RW) wake potential for the longitudinal, horizontal, and vertical planes, allowing a direct comparison to highlight the significance of the geometric contribution.

As shown in Fig. 1, over short distances, within 10 mm, the geometric wake potential is comparable to, or even slightly stronger than, the RW wake potential. Over longer distances, beyond 10 mm, the RW wake potential decays monotonically, while the geometric wake potential exhibits sustained oscillations due to trapped modes at higher frequencies excited by cavity-like structures, including gate valves and bellows. Based on this comparison, geometric impedance is expected to play a significant role in single-bunch dynamics.

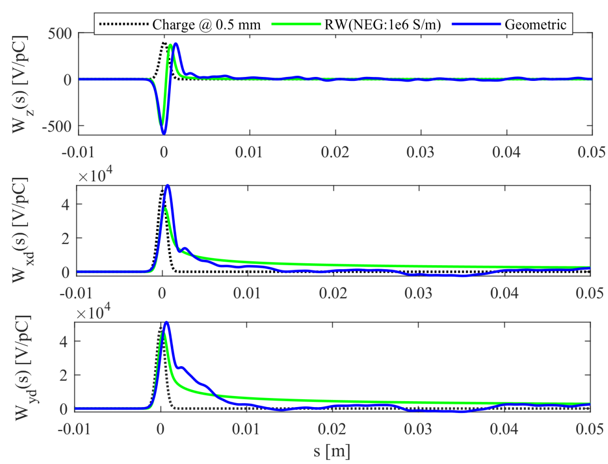

Figure 1: Total geometric and RW wake potentials for a 0.5 mm Gaussian bunch.

CONCLUSION AND OUTLOOK

Two systematic computational campaigns have established both narrow-band and broad-band impedance budgets for the HALF storage ring. The narrow-band analysis, employing a PSO-based fitting method, accurately characterized trapped modes up to 20 GHz. Key trapped-mode impedance sources are identified: gate valves dominate the longitudinal impedance, while the IVUs are the primary sources of transverse impedance, particularly in the vertical plane. The broad-band impedance budget, derived from short-range wake simulations with a 0.5 mm bunch length, is now available for single-bunch instability analysis.

Future work will focus on mitigation strategies for the gate valves and IVUs, and the established model will serve as the foundation for comprehensive beam dynamics simulations to ensure stable operation of HALF.

REFERENCES

[1] A. W. Chao, *Physics of Collective Beam Instabilities in High Energy Accelerators*. New York, NY, USA: Wiley, 1993.

[2] B. W. Zotter and S. A. Kheifets, *Impedances and Wakes in High-Energy Particle Accelerators*. Singapore: World Scientific, 1998.
doi:10.1142/3068

[3] A. Blednykh, G. Bassi, V. Smaluk, and R. Lindberg, "Impedance modeling and its application to the analysis of the collective effects", *Phys. Rev. Accel. Beams*, vol. 24, p. 104801, 2021.
doi:10.1103/PhysRevAccelBeams.24.104801

[4] R. Nagaoka and K. L. F. Bane, "Collective effects in a diffraction-limited storage ring", *J. Synchrotron Rad.*, vol. 21, no. 5, pp. 937–960, 2014.
doi:10.1107/S1600577514015215

[5] Z. Bai *et al.*, "Progress on the storage ring physics design of Hefei Advanced Light Facility (HALF)", in *Proc. IPAC'23*, Venice, Italy, May 2023, pp. 1075–1078.
doi:10.18429/JACoW-IPAC2023-MOPM038

[6] Dassault Systèmes, *CST Studio Suite*.

[7] I. Zagorodnov, *ECHO2D*.

[8] H. Yao, T. He *et al.*, "Particle swarm optimization fitting of long-range wake potentials for trapped-mode parameter characterization in the HALF storage ring", submitted for publication.